Eur Biophys J (1992) 21, 321–329

European Biophysics Journal


# Predictions of the secondary structure and antigenicity of human and bovine tropoelastins

**L. Debelle [1], S. M. Wei [2], M. P. Jacob [2], W. Hornebeck [2], and A. J. P. Alix [1]***

[1] Laboratoire de Spectroscopies et Structures Biomoléculaires, INSERM U314 – CHR Maison-Blanche, 45 rue Cognacq Jay, 51092 Reims Cedex, France
[2] Laboratoire de Biologie du Tissu Conjonctif, Faculté de Médecine, Université Paris – Val de Marne, CNRS URA 1460, 8 rue du Général Sarrail 94010 Créteil, Cedex, France

Received November 28, 1991/Accepted June 23, 1992

**Abstract.** Secondary structure and antigenicity predictive methods have been applied to the sequences of human and bovine tropoelastins in order to have some insight into the molecular structure of its insoluble counterpart, i.e., elastin. For both tropoelastins, all the predictions yielded 11 major regions, in which the pleated conformation was predominant, separated by 10 strong helical segments of various lengths located within alanyl rich regions of the chains. The overall conformations of human and bovine tropoelastins were estimated to contain $18 \pm 5\%$ $\alpha$-helices, $63 \pm 17\%$ $\beta$-sheets, $13 \pm 13\%$ $\beta$-turns and $6 \pm 6\%$ random coil. For both tropoelastins, antigenicity predictions indicated the presence of seven synthetic decapeptides corresponding to continuous linear epitopes of the molecule. Some of the predicted epitopes are located in the same regions in both species while others are not. These predictions have allowed us to propose an $\alpha/\beta$ conformation for tropoelastin. Therefore this extracellular matrix macromolecule might be more structured (10 helical segments for about 18% of the overall structure) than previously suggested.

**Key words:** Tropoelastin – Predictive methods – Secondary structure – Antigenic index – Epitope

## Introduction

The elastic properties of several tissues of vertebrates such as lung, skin and large blood vessels are mainly due to the presence, in variable quantities, of elastic fibers within their extracellular matrix (Rosenbloom 1987). Elastin, the major component of these fibers, possesses an amorphous appearance at the electron microscopic level (Ross and Bornstein 1971); it also exhibits a high intrinsic fluorescence and a great resistance to proteolysis as compared with other connective tissue proteins (Rosenbloom 1987; Thornhill 1972). Elastin is synthesized from mesenchymal cells as a soluble precursor, tropoelastin, which undergoes posttranslational modifications; in the cellular space, some of the lysine residues of tropoelastins are deaminated following the action of lysyl oxidase and cofactors (Rosenbloom 1987; Anwar and Raju 1989). A series of non-enzymatically catalysed reactions lead to the formation of specific cross-links, named desmosines, that link two chains of tropoelastin. Human tropoelastin (HTPE) is a 760 residue polypeptide with a corresponding 65.8 kDa molecular weight; bovine tropoelastin (BTPE) is very similar to its human counterpart, containing 734 residues and having a molecular weight of 62.6 kDa (Bashir et al. 1990).

In both molecules, the predominant amino acids are Gly (30%) and Ala (20%); the group of hydrophobic residues G, A, V, P, L represents 82% of the overall composition of HTPE and 83% of BTPE. G, V, P, L are equally distributed along the chains but alanines are found in clusters which also contain 1, 2 or 3 lysyl residues. Ten of these polyA-K regions are found in both tropoelastins. Other similarities between HTPE and BTPE are the absence of any Met, Asn or Trp and the presence of 2 Cys four residues apart (positions 750 and 755 for HTPE, 724 and 729 for BTPE).

However some important differences can be seen between these tropoelastins. HTPE contains twice as many Tyr, Ser and Arg residues as does BTPE and 5 Glu are present within the sequence of HTPE and none in BTPE. Finally, while BTPE does not contain any histidyl residue, HTPE has one. More generally, and whatever molecule is considered, the great majority of the residues are hydrophobic: 90% for HTPE, 91% for BTPE and more than one half of the residues belongs to the class of flexible residues. The rigid-class ones were mainly encountered in the 10 Ala-rich regions described above. In addition to the C-terminal cluster of charges found in

* *Correspondence to:* A. J. P. Alix

*Abbreviations:* HTPE, human tropoelastin; BTPE, bovine tropoelastin; AG, antigenic index; CF, Chou and Fasman algorithm; GOR, method of Garnier Osguthorpe and Robson; DC, decision constant; CD, circular dichroism; NMR, nuclear magnetic resonance

both sequences, another one can be detected in HTPE (positions 588–609) in a region very rich in flexible residues. This region is not present in BTPE.

The presence of pyridinium cross-links together with the extreme hydrophobicity of tropoelastin is responsible of the rheological properties of the polymer and its total insolubility in all solvents. These particular physicochemical properties prevent most of the usual structural investigation methods from giving significant results, so that little and somewhat contradictory information has been gathered about its secondary and tertiary structures.

The early infrared and CD studies performed by Mammi and co-workers (Mammi et al. 1968, 1970) with acid hydrolysates of elastin, i.e., α-elastins, tended to support the contention that elastin was largely disordered, although a low level of helical structures was seen. In addition, the reversible temperature elicited coacervation of soluble elastin (α-elastin), investigated by CD spectroscopy, showed that during the coacervation process, α-elastin goes from a disordered conformation to a highly helical one (50%) (Urry et al. 1969). Thus, the structure of water-swollen elastin under normal temperature conditions was considered to be mainly disordered, a view supported by NMR (Lyerla and Torchia 1975) and Raman spectroscopic data (Frushour and Koenig 1975; Prescott et al. 1987). In contrast, other investigators claimed that elastin could not be envisaged solely as a random network of mobile chains and that supramolecular organisation of the molecule might exist. Gotte et al. (1977) clearly established, using X-ray diffraction data, that elastin did contain some ordered structures. On the basis of experimental and theoretical studies of synthetic peptides, Urry proposed a regular arrangement of β-turns (β-spiral model) for the regions between the cross-links which can explain the elastic properties of the polymer when it is hydrated (Urry 1983). CD, infrared, Raman and NMR spectra of elastin-like peptides (Rahman et al. 1987; Prescott et al. 1987; Tamburro et al. 1990, 1991), CD studies of α-elastin conformational changes under different experimental conditions (Tamburro et al. 1977, 1978) and an infrared study of insoluble elastin (Renugopalakrishnan et al. 1990) have shown the β-turn conformation to be an important element in elastin structure. However, Tamburro and co-workers pointed out that the β-turns are isolated along the sequence (Tamburro et al. 1991) while in Urry's proposal they are recurrent (Urry 1983).

Thus, there are two opposed points of view regarding the location of the β-turns in the regions responsible for the elastomeric properties of the polymer, each one being related to its own theory of elastin elasticity: the β-spiral model connected to the librational entropy theory (Urry 1983) and the isolated β-turns model related to a classical elasticity mechanism (Tamburro et al. 1991). Thus the structure-elasticity relationship of elastin still remains unclear.

To some extent, the conformation of elastin is probably dictated by that of its soluble precursor; however, although the sequences of tropoelastin from different species were recently deduced from their corresponding gene product (Bashir et al. 1990), few physical measurements have been performed with the monomer owing to the difficulties of isolating material in its purified form.

Therefore, in order to have a preliminary insight into elastin structure, we took advantage of the known sequences of human and bovine tropoelastins and applied secondary structure and antigenicity predictions.

## Materials and methods

### *Secondary structure predictions*

Three standard methods of secondary structure prediction have been applied to the sequences of human and bovine (Bashir et al. 1990) tropoelastins: a statistical method, the standard Chou and Fasman algorithm with an extended data base (Argos et al. 1978) and two informational methods, the original GOR1 method of Garnier et al. (1978) and the GOR1 method modified by Busetta (1987). While the Chou and Fasman algorithm does not allow one to give any hypothesis about the structure of the sequence used, the informational GOR1 method permits one to impose certain conditions regarding the structural contents to be predicted. This can be done using a set of decision constants (DC) expressed in centinats (cnats) giving information on the folding of the polypeptide backbone (Garnier et al. 1978; Busetta 1987).

Four types of secondary substructures were used, i.e. α-helices, β-sheets, β-turns and random coil, and Table 1

**Table 1.** Names and associated hypotheses of secondary structure predictions. Decision constants are in cnats and mGOR1 refers to the modified GOR1 method (Busetta 1987)

| Name | Method | $DC_\alpha$ | $DC_\beta$ | $DC_T$ | $DC_C$ | Hypothesis |
|---|---|---|---|---|---|---|
| CF 2 | CF | None | None | None | None | None |
| GOR 0 | GOR 1 | 0 | 0 | 0 | 0 | None |
| GOR 1 | GOR 1 | 158 | 50 | 0 | 0 | $\%\alpha<20$, $\%\beta<20$ |
| GOR 2 | GOR 1 | 158 | −87.5 | 0 | 0 | $\%\alpha<20$, $\%\beta>20$ |
| GOR 3 | GOR 1 | − 75 | 50 | 0 | 0 | $20<\%\alpha<50$, $\%\beta<20$ |
| GOR 4 | GOR 1 | − 75 | −87.5 | 0 | 0 | $20<\%\alpha<50$, $\%\beta>20$ |
| GOR 5 | GOR 1 | −100 | 50 | 0 | 0 | $50<\%\alpha$, $\%\beta<20$ |
| GOR 6 | GOR 1 | −100 | −87.5 | 0 | 0 | $50<\%\alpha$, $\%\beta>20$ |
| All-β | mGOR 1 | 180 | −70 | −125 | −50 | majoritary β |
| α–β | mGOR 1 | −120 | −70 | −125 | −50 | majoritary α and β |
| All-α | mGOR 1 | −200 | 90 | −125 | −50 | majoritary α |

summarizes our structural predictions together with their DC and therefore associated hypothesis. All predictions have been deduced from CFGOR, a program developed in our laboratory and implemented on a PC.

*Antigenicity predictions*

In order to locate the major continuous epitopes of tropoelastins, we have used a new method of epitope/antigenicity prediction (Alix et al., unpublished). This method, which is an extension and combination of the methods of Parker et al. (1986) and of Jameson and Wolf (1988), yields a composite surface profile used as antigenic index (AG), the calculation of which is briefly summarized below.

Four classes of basic biophysical parameters are considered for AG determination. The first class to be considered is the type of secondary substructure of residues predicted using CF2 and GOR0 (Argos et al. 1978; Garnier et al. 1978). Only the $\beta$-turn and coil conformations are considered to be favorable for antigenicity and thus the residues predicted in these conformations are the more likely to be antigenically predicted.

The second class of parameters considered is the hydropathy of residues. Three scales were used (Hopp and Woods 1981; Kyte and Doolittle 1982; Parker et al. 1986). A residue is more likely to be antigenic if it is predicted to be in an hydrophilic environment, and less likely if it is in an hydrophobic one, each scale being considered separately. Thus, in each scale, the hydrophilic residues will raise the final AG value, while the hydrophobic ones will lower it.

The third class is the surface accessibility of residues. Two scales were used: the fractional probabilities of Emini et al. (1985) modified by Alix et al. (unpublished) and the interior to surface transfer energy (Janin 1979). Each prediction is treated independently, and the residues predicted as surface accessible are considered more likely to be antigenic.

The last class concerns the flexibility of residues (Karplus and Schulz 1985), with the flexible residues more likely to be antigenic.

Thus, in each class of parameters, each individual prediction obtained is filtered and/or smoothed to give a specific profile; in the same class, these specific profiles are then averaged to give a class profile. The antigenic index profile is computerized as a linear combination of the four class profiles: the secondary structure accounts for 40% of the index, the hydropathy for 30%, and both the surface accessibility and the flexibility of residues for 15% (Jameson and Wolf 1988). The higher the value of AG for a residue, the more likely is it to be part of a continuous linear epitope.

Prior to giving the final ordered predictions, our results have been compared and/or correlated with several other predictions and these specific parameters are: polarity, other scales of hydrophobicity, free energy of transfer, hydration potential, radial location of residues, antigenic values... (Cornette et al. 1987; Schulz 1988) and especially to the surface protruding regions of the molecules predicted by the calculation of their protrusion index (Thornton et al. 1989), since this method is directly derived from molecular graphics and crystallography.

In principle, the AG method is similar to that of Jameson and Wolf (1988); however, it is a more restrictive method. Indeed, although the antigenic index of Jameson and Wolf is calculated with the same classes (structure, hydropathy, surface accessibility and flexibility), our method considers several uncorrelated scales in each class (Cornette et al. 1987) while the former did not. In addition, among the scales we used, several have already been tested individually and proved to be well adapted for locating continuous epitopes in proteins (Van Regenmortel and Daney de Marcillac 1988). Therefore, our AG method consists of a restriction of previous predictions. Furthermore, since our final data are not smoothed, much less information is lost. Our AG determination is able to predict fewer epitopes for a given protein than the algorithm of Jameson and Wolf but when tested with known epitopes, it gave better agreement (Alix et al., unpublished).

Finally, the sequences of HTPE and BTPE have been compared in order to locate predicted epitopes along the chains and to check whether any of them can be recovered in both molecules.

## Results

*Secondary structure predictions*

Four types of secondary substructures, i.e. $\alpha$-helices, $\beta$-sheets, $\beta$-turns and random coil, were assigned for the whole length of the tropoelastin molecules. The quantitative results for both HTPE and BTPE are given in Table 2 and show that whatever method used, the structural contents of HTPE and BTPE are quite similar. However, the GOR 1, 3, 5 and 6 predictions, as well as the all-$\alpha$ type one of Busetta (1987) were rejected since the numerical predictions did not agree with the hypothesis imposed by the decision constants (Table 1). A similar criticism could be

**Table 2.** Quantitative secondary structure predictions for HTPE and BTPE

| Predictions | HTPE | | | | BTPE | | | |
|---|---|---|---|---|---|---|---|---|
| | %$\alpha$ | %$\beta$ | %T | %C | %$\alpha$ | %$\beta$ | %T | %C |
| CF 2 | 23 | 27 | 20 | 30 | 23 | 30 | 19 | 28 |
| GOR 0 | 20 | 55 | 10 | 15 | 19 | 54 | 10 | 17 |
| GOR 1 | 16 | 39 | 15 | 30 | 16 | 38 | 14 | 32 |
| GOR 2 | 13 | 80 | 4 | 3 | 13 | 78 | 4 | 5 |
| GOR 3 | 25 | 35 | 14 | 26 | 21 | 36 | 14 | 29 |
| GOR 4 | 21 | 73 | 3 | 3 | 20 | 72 | 4 | 4 |
| GOR 5 | 26 | 35 | 13 | 26 | 22 | 36 | 13 | 29 |
| GOR 6 | 22 | 72 | 3 | 3 | 21 | 71 | 4 | 4 |
| All-$\beta$ | 13 | 51 | 30 | 6 | 13 | 53 | 28 | 6 |
| $\alpha-\beta$ | 22 | 45 | 28 | 5 | 20 | 48 | 27 | 5 |
| All-$\alpha$ | 28 | 4 | 48 | 20 | 24 | 4 | 55 | 17 |

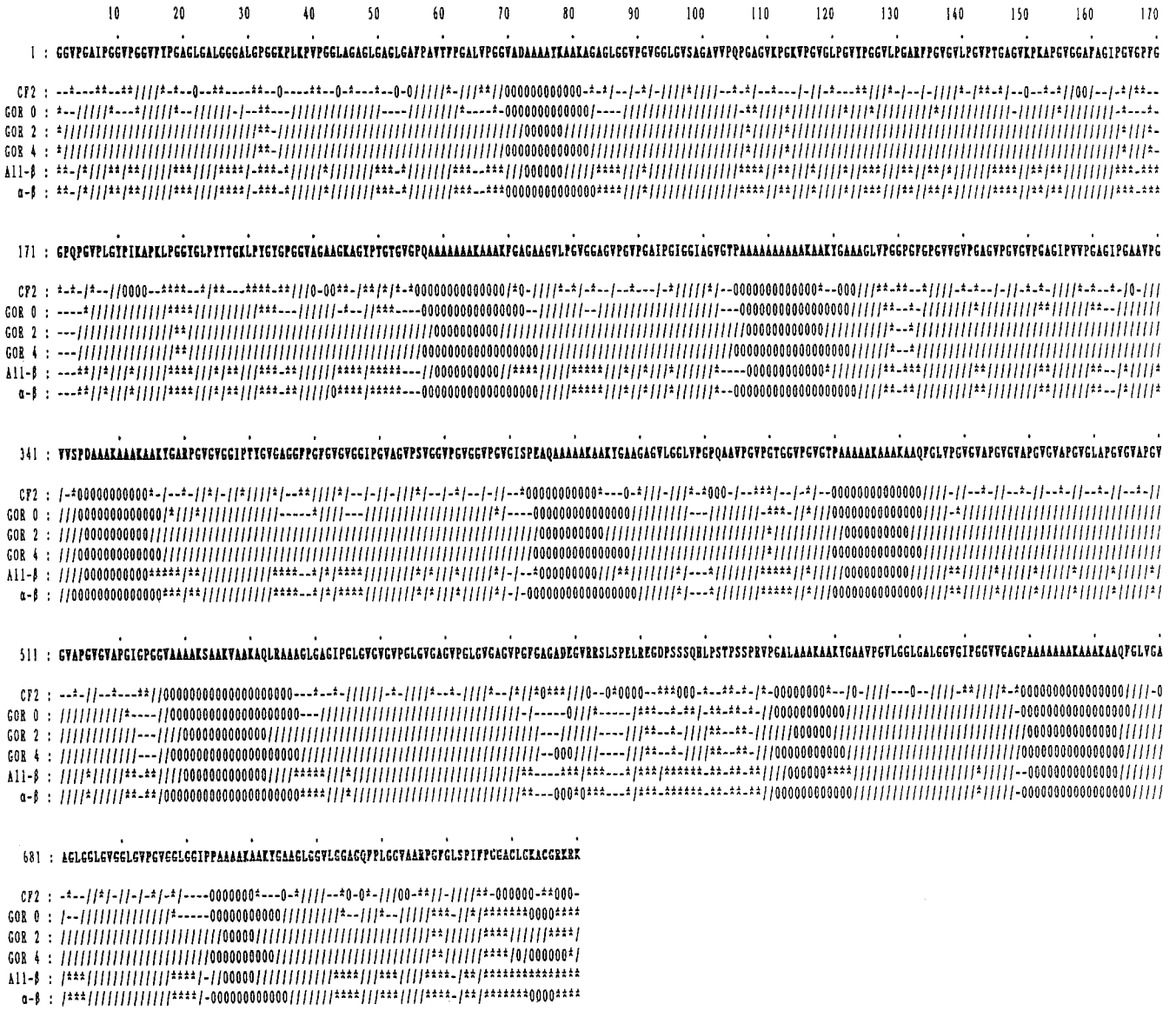

**Fig. 1.** Predicted secondary structure assignments for HTPE. 0, helix; /, sheet; *, turn; –, coil. Each predicted structure row has the name of its parent prediction (see Table 2)

put forward for the $\alpha-\beta$ type prediction although it gave high levels of helical and pleated contents and figures similar to the all-$\beta$ type.

Accordingly, a set of six predictions was retained for each tropoelastin and the corresponding secondary structure assignments for HTPE are shown in Fig. 1. The CF2 prediction showed an overall structure of HTPE where the protein was composed of 11 major regions whose structure was undefined, being an irregular mixture of all substructures, separated by 10 well defined helices corresponding to the Ala-rich segments of the molecule. GOR 0, GOR 2 and GOR 4 predictions also indicated the presence of similar regions. However, the helices had various lengths depending on the prediction, and the 11 regions were found to be mainly in the pleated conformation with $\beta$-sheets of variable length depending on the decision constants used. In the case of GOR 0, they are relatively short (usually 4–10 residues) and separated by either turn or coil residues while in the GOR 2 and GOR 4 predictions they are much longer (up to 60 residues) covering nearly the entire length between the helical segments. In contrast, the all-$\beta$ and $\alpha-\beta$ predictions yield different structures for these regions in HTPE. In most cases, the pleated segments appeared to be of limited length and were most often separated by six turn or coil residues; interestingly the great majority of the sequence exhibited a similar local structure arrangement with the exception of those regions bordering the predicted helices. The GOR 1 method takes into account a broader neighbourhood of residues than CF2, so it is probably more accurate than the other predictions and it should be considered carefully. Thus, if all the numerically valid predictions except CF2 are considered and averaged, tropoelastin of either human or bovine origin would be constituted of $18\pm5\%$ $\alpha$-helices, $63\pm17\%$ $\beta$-sheets, $13\pm13\%$ $\beta$-turns and $6\pm6\%$ random coil. The

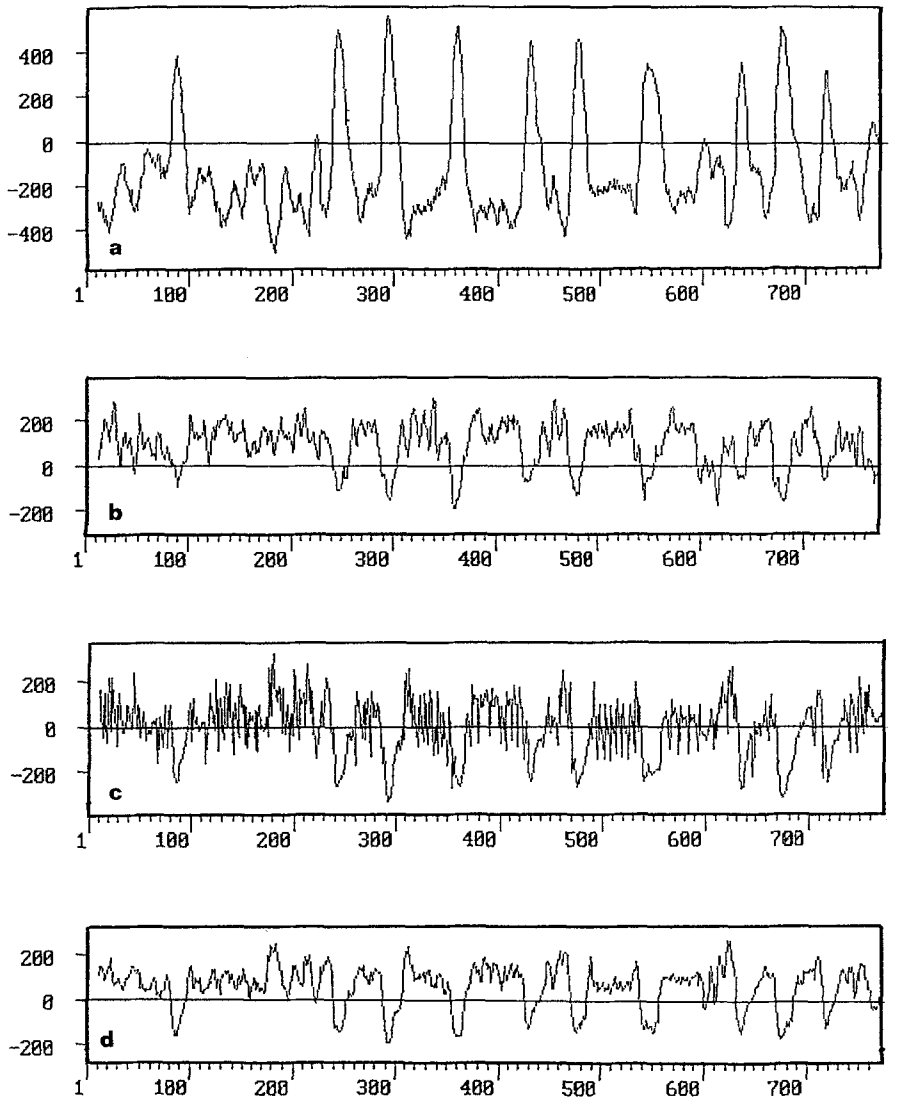


**Fig. 2.** Plots of predictions for the substructures used in the case of the GOR 0 prediction for HTPE. a, helices; b, sheets; c, turns; d, coil. X axes show the HTPE sequence; Y axes are graduated in centinats

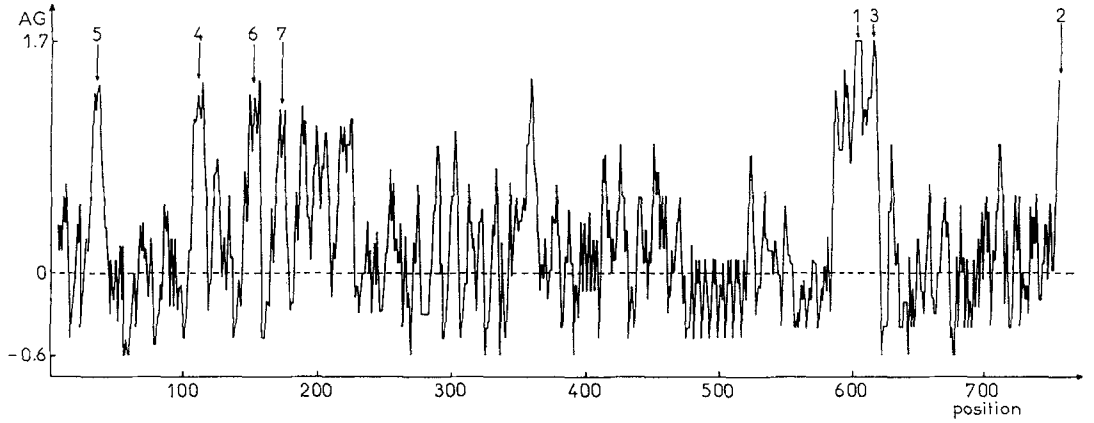


**Fig. 3.** Antigenic index plot for HTPE. Abscissa, sequence; ordinate, AG value. The peak marks indicate the antigenicity confidence order

deviations are acceptable for the helical and extended conformations but show that the turn and coil ones are badly determined.

The prediction for each substructures has been plotted for the GOR 0 prediction of HTPE (Fig. 2) in order to show what are the structural contributions in each region of the sequence. The helices are unambiguously predicted (Fig. 2a). However, as can be seen in Figs. 2b–d, in the other regions of the molecule the predictions for the non-helical substructures share similar profiles and close val-

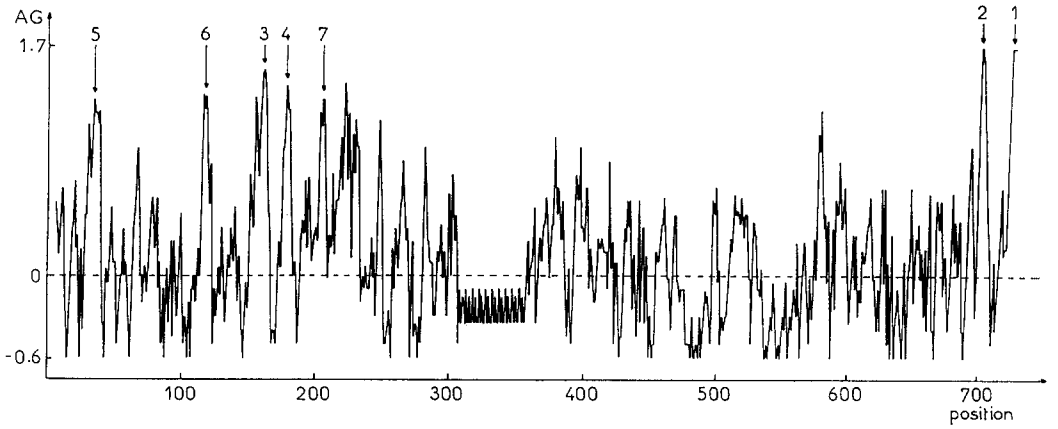


**Fig. 4.** Antigenic index plot for BTPE. Abscissa, sequence; ordinate, AG value. The peak marks indicate the antigenicity confidence order

**Table 3.** Predicted antigenic decapeptides of HTPE and BTPE as a decreasing function of their antigenic confidence order. AG values of 1.7 are indicated by bold face. The protruding segments predicted by the method of Thornton et al. (1989) are marked with an asterix

| Order | HTPE | | BTPE | |
|---|---|---|---|---|
| | Positions | Segment | Positions | Segment |
| 1 | 600–609 | **REGDPSSSQH*** | 725–734 | LGKS**CGRKRK** |
| 2 | 751–760 | LGKAC**GRKRK*** | 702–711 | VGG**KP**PKPFG* |
| 3 | 610–619 | LPSTPSSPRV* | 156–165 | AGVKPKAPGG* |
| 4 | 106–115 | PGAGVKPGKV* | 177–186 | PFGGQQPGVP |
| 5 | 29– 38 | ALGPGGKPLK* | 33– 42 | GVKPAKPGVG |
| 6 | 147–156 | AGVKPKAPGV | 114–123 | GAGVKPGKVP* |
| 7 | 168–177 | PFGGPQPGVP | 202–211 | LPYKTGKLPY |

ues at each point, with only a slight numerical bias towards the pleated conformation.

More generally, what holds for HTPE is also valid for BTPE (data not shown but available on request). Here again, 10 helices of various lengths are predicted, which separate the molecule into 11 large regions where the predominant structure seems to be the pleated one. One exception concerns the 590–620 region of the human sequence which has no equivalent in BTPE.

*Antigenicity predictions*

The final composite profile of the epitope/antigenic indices of HTPE and BTPE are plotted in Figs. 3, 4 respectively. For both molecules, well defined and highly antigenic (AG > 1) regions were found in both N and C-terminal parts of the tropoelastins. Several rather short sequences (1–3 residues) with high indices were also encountered in the middle part of the proteins. Quite remarkably the 590–620 sequence of HTPE exhibits a very high antigenic index.

To be a good potential epitope, a peptide sequence should exhibit a high AG value associated with a clear peak in the final composite profile. Table 3 presents the ordered antigenic predictions for HTPE and BTPE in the

```
HTPE    1  GGVPGAIPGGVPGGVFYPGAGLGALGGGALGPGGKPLKPVPGGLAGAGLG  50
BTPE    1  GGVPGAVPGGVPGGVFFPGAGLGGLGVGGLGPGVKPAKPGVGGLVGPGLG  50

HTPE   51  AGLGAFPAVTFPGALVPGGVADAAAAYKAA-KAGA---GLGGVPGVGGLG  96
BTPE   51  AGLGALPGA-FPGALVPGGPAGAAAAYKAAAKAGAAGLGVGGIGGVGGLG  99

HTPE   97  VSAGAVVPQPGAGV-----KPGKVPGVGLPGVYPGGVLPGA--RFPGVGVL  140
BTPE  100  VSTGAVVPQLGAGVGAGVKPGKVPGVGLPGVYPGGVLPGAGARFPGIGVL  149

HTPE  141  PGVPTGAGVKPKAPGVGGAFAGIPGVGPFGGPQPGVPLGYPIKAPKLPGG  190
BTPE  150  PGVPTGAGVKPKAPGGGGAFAGIPGVGPFGGQQPGVPLGYPIKAPKLPAG  199

HTPE  191  YGLPYTTGKLPYGYGPGGVAGAAGKAGYPTGTGVGPQAAAAAAAKAAAKF  240
BTPE  200  YGLPYKTGKLPYGFGPGGVAGSAGKAGYPTGTGVGPQAAAAAA-KAAAKL  248

HTPE  241  GAGAAGVLPGVG--GAGVPGVPGAIPGIGGIAGVGTPAAAAAAAAAAKAA  288
BTPE  249  GAGGAGVLPGVGVGGAGIPGAPGAIPGIGGIAGVGAPDAAAAAAAAAKAA  298

HTPE  289  KYGAAAGL-VPGGPGFGPGVVGVPGAGVPGVGVPGAGIPVV---------  328
BTPE  299  KFGAAGGFPGVGVPGVGVPGVGVPGVGVPGVGVPGVGVPGVGVPGVPG  348

HTPE  329  ---PGAGIPGAAVPGVVSPEAAAKAAAKAAKYGARPGVGVGGIPTYGVGA  375
BTPE  349  VGVPGVGVPGVGVPGAVSPAAAAKAAAKAAKFGARGGVGIGGIPTFGVGP  398

HTPE  376  GGFPGFGVGVGGIPGVAGVPSVGGVPGVGGVPGVGISPDAQAAAAAKAAK  425
BTPE  399  GGFPGIGDAAA----------------------------AQAAAAAKAAK  420

HTPE  426  YGAAGAGVLGGLVPGPQAAVPGVPGTGGVPGVGTPAAAAAKAAAKAAQFG  475
BTPE  421  IGAGGVGALGGLVPGAPGAIPGVPGVGGVPGVGIPAAAAAKAAAKAAQFG  470

HTPE  476  LVPGVGVAPGVGVAPGVGVAPGVGLAPGVGVAPGVGVAPGVGVAPGIGPG  525
BTPE  471  LGPGVGVAPGVGVVPGVGVVPGVGVAPGIGLGPGGVIGAGV---------  511

HTPE  526  GVAAAAKSAAKVAAKAQLRAAAGLGAGIPGLGVGVGVPGLGVGAGVPGLG  575
BTPE  512  --PAAAKSAAKAAAKAQFRAAAGLPAGVPGLGVGVGVPGLGVGVGVPGLG  559

HTPE  576  VGAGVPGFGAGADEGVRRSLSPELREGDPSSSQHLPSTPSSPRVPGALAA  625
BTPE  560  VGAGVPGFGA----------------------------------VPGTLAA  576

HTPE  626  AKAAKYGAAVPGVLGGLGALGGVGIPGGVVGAGPAAAAAAAKAAAKAAQF  675
BTPE  577  AKAAKFGPGGVGALGGVGDLGGAGIPGGVAGVGPAAAAAA-KAAAKAAQF  625

HTPE  676  GLVGAAGLGGLGVGGLG-VPGVGGLGGIPPAAAAKAAKYGAAGLGGVLGG  724
BTPE  626  GL---GGVGGLGVGGLGAVPGAVGLGGVSPAAAAKAAKFGAAGLGGVLGA  672

HTPE  725  AGQFPLGGVAARPGFGLSPIFPGGA-------------------------  749
BTPE  673  GQPFPIGGVAARPGFGLSPIFPGGAGGLGVGGKPPKPFGGALGALGFPGG  722

HTPE  750  -CLGKACGRKRK  760
BTPE  723  ACLGKSCGRKRK  734
```

**Fig. 5.** Comparison of HTPE and BTPE sequences. The comparison criterion used is the genetic code; –, gap. The bold underlined segments show the antigenic predicted decapeptides

form of synthetic decapeptides predicted to correspond to linear continuous epitopes of the molecule. They are given in decreasing order of their antigenic index values and thus antigenicity confidence. For either BTPE or HTPE, decapeptides at the COOH terminal part of the molecule

do exhibit high antigenic probability, and there is a good correlation between our antigenic predictions and the protruding regions of the molecules predicted by the method of Thornton et al. (1989).

The genetic code was further used as a comparison criterion (Fig. 5). The alignment of the two tropoelastins clearly showed that some predicted antigenic decapeptides overlapped. However, some did not; this is especially true for the human 600–609 and 610–619 segments which are both absent in the bovine sequence. Thus it seemed reasonable to assume that these peptides might confer species specificity to the antigenic response.

## Discussion

Although the structures of elastin and α-elastin have been extensively studied, that of tropoelastin has not because it is difficult to obtain in large amounts. Thus, the conformation of tropoelastin remains unknown as no X-ray, NMR or other structural data are available in the literature. However a CD study of chick tropoelastin in the presence of different agents showed that the molecule could be somewhat structured. Furthermore, in the presence of sodium dodecyl sulfate 20–25% of the residues were in a helical conformation (Rucker et al. 1973).

In this investigation, several calculation methods have been applied in order to predict the conformations of tropoelastins from human and bovine sources. Independent of the method of calculation, our data demonstrate the presence of 10 helical segments concentrated within the potential cross-linking domains of tropoelastins; the remainder of the molecule was assigned mainly to the pleated conformation using the GOR 1 prediction method, while in the CF 2 predictions the 11 major regions of the molecule were predicted to be almost equally in the pleated, turn and coil conformations. Although some ordered structures were also seen in the COOH terminal region of the molecule, it has to be emphasized that for most proteins, terminal COOH or $NH_2$ domains are often very flexible and unstructured. Knowing that the GOR 1 method is more accurate than the CF one, we propose the following structural contents for both tropoelastins: $18 \pm 5\%$ α-helices, $63 \pm 17\%$ β-sheets, $13 \pm 13\%$ β-turns and $6 \pm 6\%$random coil. However, if this structural estimation might seen acceptable for tropoelastin, it has to be reconsidered in the context of its polymeric form, i.e. insoluble elastin, and the question is raised of whether or not these methods can predict the structure of a protein such as tropoelastin. Indeed a molecule containing so much ordered structure can hardly be considered to possess elastomeric properties, even in its polymerized form.

Data used in our predictions are derived from crystallography, so that here tropoelastin has to be considered in the solid state and the influence of water on the conformation of the molecule is not taken into account. This point is noteworthy since infrared spectroscopy has shown that water forms very strong hydrogen bonds with elastin (Bertoluzza et al. 1989). In addition, the regions between the cross-links are very mobile in elastin and α-elastin (Lyerla and Torchia 1975; Tamburro et al. 1991). It seems therefore reasonable to assume that they may share similar properties in hydrated tropoelastin. Since prediction curves for β-turn, pleated or random conformations are very close (Fig. 2), a minor motion of the peptide backbone could induce a local conformation change. Thus, it is highly probable that a dynamic equilibrium could exist between these three substructures, an equilibrium where structural water might have a crucial role.

Other investigations (Guantieri et al. 1980; Tamburro et al. 1982) have shown that α-elastin exhibits CD features characteristic of a β-structure when interacting with bile salts. The displacement of structural water by such hydrophobic compounds might be responsible for the stabilisation of the "original" pleated structure. In this way, the overall equilibrium could be pulled towards an extended conformation and the CD spectrum of the degraded polymer would then exhibit β-structure characteristics.

It has to be assumed that CD spectra of all-β proteins whose β-sheets are either very short and irregular or very much distorted do resemble spectra of random coil models (Manavalan and Johnson 1983). The CD spectrum of α-elastin is typical of a random coil model (Urry et al. 1969).

Therefore, the 11 major regions of the molecule we have predicted might be constituted of short to medium size β-sheets separated by unordered and/or turn conformations in the solid state. If this is the case, then the conformation of the anhydrous molecule would consist of pleated segments linked by turn and/or coil residues alternating with helices (about 18 percent of the overall conformation). This would classify tropoelastin as an α/β class protein, on the edge of being an all-β one because of its very large content of extended conformation (Levitt and Chothia 1976). Thus, with the qualifications we have developed earlier, we suggest the following structural estimations for anhydrous HTPE and BTPE:

α-helices $18 \pm 5\%$, β-sheets $63 \pm 17\%$, β-turns $13 \pm 13\%$ and random coil $6 \pm 6\%$.

It has to be emphasized however that the proposed tropoelastin structure is acceptable only when tropoelastin is considered in its solid state, that is a molecule constituted of alternating α-helical and mainly pleated regions with short to medium β-sheets separated either by β-turns or some coiled residues. In this sense, our structural model supports the isolated β-turns model for elasticity (Tamburro et al. 1991).

Our antigenic predictions led us to delineate a series of decapeptides with high AG values. The strong antigenicity of the COOH terminal end of tropoelastin has already been reported (Rosenbloom et al. 1986), and recent investigations by some of us demonstrated that such antigenic determinants are still present in alkaline hydrolyzates and purified insoluble elastin (Wei et al., unpublished). It was recently suggested that antibodies raised against the VGVAPG hexapeptide, a sequence that recognized the elastin receptor and which is repeated 6 times in HTPE and 3 times in BTPE, react with tropoelastin and its polymer (Wrenn et al. 1986). However we have not pre-

dicted that repetitive peptide as a possible epitope for tropoelastins mainly because it was predicted to be in a pleated conformation and it is highly hydrophobic. Nevertheless, the VGVAPG sequence nearest to the COOH terminus was predicted to be more surface accessible and more flexible than the other repeats.

Although our AG method regards hydrophobicity as a negative factor for antigenicity, hydrophobic segments of a molecule can be selected as potentially antigenic (Alix et al., unpublished). Thus, we think that our method does not overestimate the importance of hydrophobicity in terms of antigenicity but rather that molecule-receptor interactions should not be envisaged as antibody-antigen recognition although some parameters associated with antigenicity could be applied individually to antigen-antibody interaction.

Again, we would like to underline that all our predictions are intended for tropoelastin and may not be entirely revelant for its insoluble counterpart. Indeed, a great number of the peptides predicted to be antigenic contain lysyl residues in their sequence, one of the reasons for their high AG. Since the great majority of these residues are involved in the formation of cross-links during elastogenesis, the antigenicity of these peptides will undoubtedly be affected in insoluble elastin.

However, if the AG values of these areas and the pleated conformation content of the molecule might be different after polymerization, we speculate that the Ala-rich regions would still keep an α-helical conformation in insoluble elastin. First it has to be emphasized that lysyl residues have side chains located far away from the peptide backbone, so that any local conformational change induced by desmosine or lysinonorleucine formation should be minimal. Secondly, the amount of information (in cnats) in favour of helical conformation is overwhelming when compared to other information values in these Ala-rich regions (Fig. 2). Thirdly, and as we pointed out, the alanyl residues in these cross-linked areas of the elastin molecule belong to the rigid class and therefore would undoubtedly resist any conformational change. This provides these regions with a locally rigid helical conformation which probably play a key role in elastogenesis.

Bashir and his colleagues have demonstrated that exon 33 of both the HTPE and BTPE genes is alternatively spliced (Bashir et al. 1990). Therefore we have investigated what might be the influence of the changes in tropoelastin sequence on our results. Both secondary structure and antigenic predictions for either modified molecule did not show any major difference when the sequence corresponding to exon 33 was missing. Thus the structural and functional implications of these tropoelastin isoforms where exon 33 is spliced still remain uncertain (Boyd et al. 1991).

These preliminary predictive results have now to be compared with results from optical spectroscopy in order to better describe the elastin molecule. This work is under progress and preliminary investigations (CD spectra of BTPE) have suggested that our structural model of tropoelastin might be representative of the BTPE conformation in solution (Debelle et al., unpublished observations).

## References


Anwar RA, Raju K (1989) Bovine elastin A, B, and C. In: Robert L and Hornebeck W (eds) Elastin and elastases, Vol. II. CRC Press, Boca Raton, pp 243–254

Argos P, Hanei M, Garavito RM (1978) The Chou-Fasman secondary structure prediction method with an extended data base. FEBS Lett 93:19–24

Bashir M, Indik Z, Yeh H, Abrams W, Ornstein-Goldstein N, Rosenbloom JC, Fazio M, Uitto J, Mecham R, Rosenbloom J (1990) Elastin gene structure and mRNA alternative splicing. In: Tamburro AM and Davidson JM (eds) Elastin, chemical and biological aspects. Congedo Editore, Galatina, pp 45–70

Bertoluzza A, Bonora S, Fini G, Morelli MA (1989) Spectroscopic studies of connective tissues: native and hydrated elastin. Can J Spectro 34:13–14

Boyd CD, Christiano AM, Pierce RA, Stolle CA, Deak SB (1991) Mammalian tropoelastin: multiple domains of the protein define an evolutionarily divergent amino acid sequence. Matrix 11:235–241

Busetta B (1987) The use of folding patterns in the prediction of protein topologies. Biochem Biophys Acta 916:54–65

Cornette JL, Cease KB, Margalit H, Spouge JL, Berzofsky JA, DeLisi C (1987) Hydrophobicity scales and computational techniques for detecting amphipatic stuctures in proteins. J Mol Biol 195:659–685

Emini E, Hughes JV, Perlow DS, Boger J (1985) Induction of hepatitis A virus-neutralizing antibody by a virus-specific synthetic peptide. J Virol 55:836–839

Frushour BG, Koenig JL (1975) Raman scattering of collagen, gelatin, and elastin. Biopolymers 14:379–391

Garnier J, Osguthorpe DJ, Robson B (1978) Analysis of the accuracy and implications of simple methods for predicting the secondary structure of globular proteins. J Mol Biol 120:97–120

Gotte L, Mammi M, Pezzin G (1977) Some structural aspects of elastin revealed by X-ray diffraction and other physical methods. In: Sandberg LB, Gray WR and Franzblau C (eds) Elastin and elastic tissue. Adv Exp Med Biol 79. Plenum Press, New York, pp 236–245

Guantieri V, Tamburro AM, Daga-Gordini D (1980) Conformational changes induced in α-elastin by cholesterol, taurocholate and unsaturated fatty acids. Int J Biol Macromol 2:68–72

Hopp TP, Woods KR (1981) Prediction of antigenic determinants from amino acid sequences. Proc Natl Acad Sci USA 78:3824–3828

Jameson BA, Wolf H (1988) The antigenic index: a novel algorithm for predicting antigenic determinants. CABIOS 4:181–186

Janin J (1979) Surface and inside volumes in globular proteins. Nature 277:491–492

Karplus PA, Schulz GE (1985) Prediction of chain flexibility in proteins, a tool for the selection of peptide antigens. Naturwissenschaften 72:212–213

Kyte J, Doolittle RF (1982) A simple method for displaying the hydropathic character of a protein. J Mol Biol 157:105–132

Levitt M, Chothia C (1976) Structural patterns in globular proteins. Nature 261:552–557

Lyerla JR, Torchia DA (1975) Molecular mobility and structure of elastin deduced from the solvent and temperature dependence of $^{13}C$ magnetic resonance relaxation data. Biochemistry 14:5175–5183

Mammi M, Gotte L, Pezzin G (1968) Evidence for order in the structure of α-elastin. Nature 220:371–373

Mammi M, Gotte L, Pezzin G (1970) Comparison of soluble and native elastin conformations by far-ultraviolet circular dichroism. Nature 225:380–381

Manavalan P, Johnson Jr WC (1983) Sensitivity of circular dichroism to protein tertiary structure class. Nature 305:831–832

Parker JMR, Guo D, Hodges RS (1986) New hydrophilicity scale derived from high-performance liquid chromatography peptide retention data: correlation of predicted surface residues with

antigenicity and X-ray-derived accessible sites. Biochemistry 25:5426–5432

Prescott B, Renugopalakrishnan V, Thomas Jr GJ (1987) Raman spectrum and structure of elastin in relation to type-II β-turns. Biopolymers 26:934–936

Renugopalakrishnan V, Riggle CJ, Jakobsen RJ, Keith DA (1990) Elastin: a glimpse of the secondary structure in the solid state from vibrational spectroscopic studies. In: Tamburro AM and Davidson JM (eds) Elastin, chemical and biological aspects. Congedo Editore, Galatina, pp 155–166

Rahman SA, Elsafty M, Hattaba A (1987) A circular dichroism and infrared study of β-turn formation in repeat peptides of elastin. Oriental J Chem 3:40–45

Rosenbloom J (1987) Elastin: an overview. Meth Enzym 14:172–196

Rosenbloom J, Weinbaum G, Abrams W, Ornstein-Goldstein N, Indik Z, Kucich U (1986) Newly determined carboxy terminal sequences in tropoelastin: immunologic identification in insoluble elastin. Collagen Rel Res 6:423–433

Ross R, Bornstein P (1971) Elastic fibers in the body. Scientific American 224:44–52

Rucker RB, Goettlich-Rieman W, Tom K (1973) Properties of chick tropoelastin. Biochem Biophys Acta 317:193–201

Schulz GE (1988) A critical evaluation of methods for prediction of protein secondary structures. Ann Rev Biophys Chem 17:1–21

Tamburro AM, Guantieri V, Daga-Gordini D, Abatangelo G (1977) Conformational transitions of α-elastin. Biochem Biophys Acta 492:370–376

Tamburro AM, Guantieri V, Daga-Gordini D, Abatangelo G (1978) Concentration-dependant conformational transition of α-elastin in aqueous solution. J Biol Chem 253:2893–2894

Tamburro AM, Guantieri V, Daga-Gordini D (1982) Human α-elastins: lipid-induced conformational changes. Int J Biol Macromol 4:111–115

Tamburro AM, Guantieri V, Pandolfo L, Scopa A (1990) Synthetic fragments and analogues of elastin. II. Conformational studies. Biopolymers 29:855–870

Tamburro AM, Guantieri V, Scopa A, Drabble JM (1991) Polypeptide models of elastin: CD and NMR studies on synthetic poly(X-Gly-Gly). Chirality 3:318–323

Thornhill DP (1972) Elastin: locus and characteristics of chromophore and fluorescence. Conn Tissue Res 1:21–30

Thornton JM, Barlow DJ, Edwards MS (1989) Antigenic recognition. In: Graham Richards W (ed) Computer-aided molecular design. IBC Technical Services Ltd, London, pp 187–196

Urry DW, Starcher B, Partridge SM (1969) Coacervation of soluble elastin effects a notable conformational change. Nature 222:795–796

Urry DW (1983) What is elastin; what is not. Ultrastr Path 4:227–251

Van Regenmortel MHV, Daney de Marcillac G (1988) An assessment of prediction methods for locating continuous epitopes in proteins. Immunol Lett 17:95–108

Wrenn DS, Griffin GL, Senior RM, Mecham RP (1986) Characterization of biologically active domains on elastin: identification of a monoclonal antibody to a cell recognition site. Biochemistry 25:5172–5176